LBL-35308
UC-410

Lawrence Berkeley Laboratory
UNIVERSITY OF CALIFORNIA

Materials Sciences Division

Presented at the POLIMEX '93 Symposium,
Cuncum Quintana Roo, Mexico, November 1–3,
1993, and to be published in the Proceedings

Nonlinear Optical Studies of Polymer Interfaces

Y.R. Shen

November 1993

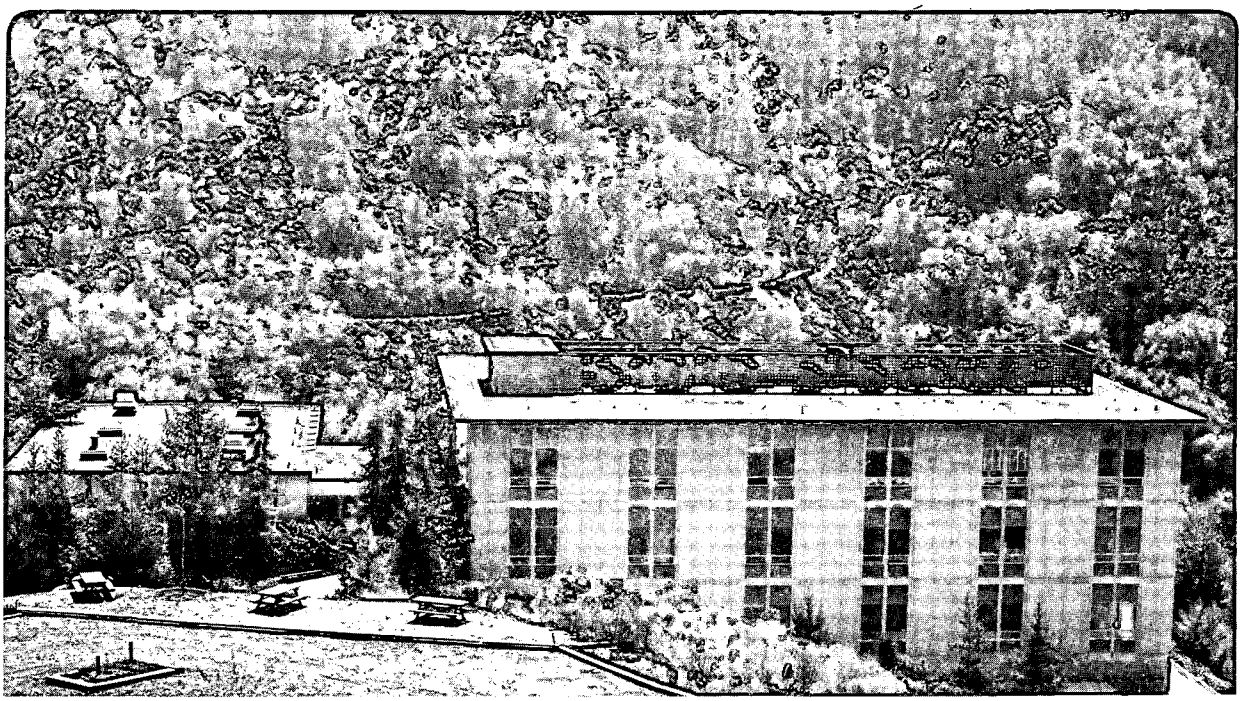

Prepared for the U.S. Department of Energy under Contract Number DE-AC03-76SF00098

DISCLAIMER

LBL-35308
UC410

Nonlinear Optical Studies of Polymer Interfaces

Y. R. Shen

Department of Physics
University of California

and

Materials Sciences Division
Lawrence Berkeley Laboratory
University of California
Berkeley, California 94720

November 1993

This work was supported by the Director, Office of Energy Research, Office of Basic Energy Sciences, Materials Sciences Division, of the U.S. Department of Energy under Contract No. DE-AC03-76SF00098.

LBL-35308
UC410

NONLINEAR OPTICAL STUDIES OF POLYMER INTERFACES

Y. R. Shen

Department of Physics, University of California, and
Materials Sciences Division, Lawrence Berkeley Laboratory,
Berkeley, California 94720

Abstract

Second-order nonlinear optical processes can be used as effective surface probes. They can provide some unique opportunities for studies of polymer interfaces. Here we describe two examples to illustrate the potential of the techniques. One is on the formation of metal/polymer interfaces. The other is on the alignment of liquid crystal films by mechanically rubbed polymer surfaces.

In recent years, the possibility of employing nonlinear optical effects as surface diagnostic tools has attracted a great deal of attention. Optical second harmonic generation (SHG) and sum frequency generation (SFG), in particular, have been developed into effective versatile probes for surface and interface studies.[1] As second-order nonlinear optical processes, they are forbidden in media with inversion symmetry, but necessarily allowed at surfaces and interfaces. As a result, they are highly surface specific.[2] In comparison with other surface analytical tools, they have the advantages of being capable of high spatial, temporal, and spectral resolutions, suitable for *in-situ*, remote sensing of samples in hostile environment, and applicable to all interfaces accessible by light.

SHG from a boundary surface was first studied theoretically by Bloembergen and Pershan in 1962.[3] Experimental studies to compare with theory were subsequently carried out by many researchers.[4] Attention was then drawn to the problem of understanding the physical origin of nonlinearities responsible for the surface SHG.[5] There were experimental evidences that SHG

could be highly surface sensitive.[6] They were however largely ignored. Not until 1980 was the surface sensitivity of SHG rediscovered and the possibility of using SHG for surface studies truly explored. This happened when surface enhanced Raman scattering (SERS) became a hot topic for investigation. It was first found by Fleischmann *et al.*[7] that for molecules adsorbed on clustered silver surfaces, the Raman intensity could increase by ~10^6. It was believed by many researchers that the effect is mainly due to surface local field enhancement arising from plasma resonance on the clusters. One should then expect, for the same reason, strong enhancement of SHG from the same surfaces. Indeed this was found to be the case,[8] and adsorption and desorption of molecular monolayers on such surfaces could be detected.[9] The signal was so strong that even without surface enhancement, it could have been easily measured. This led to subsequent experiments studying monolayer adsorbates on smooth surfaces and the development of SHG and SFG as surface probes.[1]

SHG and SFG have already been applied with great success to a large variety of surface and interfacial problems:[1] probing adsorption and desorption of molecules from surfaces, measuring average molecular orientation and arrangement of adsorbates, monitoring surface symmetry and surface phase transitions, conducting surface microscopy and spectroscopy, and many others. In this paper, we shall describe a few experiments carried out on polymer interfaces using SHG.

We first discuss the application of SHG to study the formation dynamics of copper/polyimide interfaces.[10] In recent years, polymer/metal interfaces have become an important area of research. Interdiffusion of species at a metal/polyimide interface appears to play an important role in controlling the properties of the interface. Several advanced techniques have been used for these diffusion studies, such as Rutherford backward scattering (RBS),[11] transmission electron microscopy (TEM),[12] and radiotracer(RT) technique in combination with low energy ion sputtering.[12] The accuracy of these measurements is often limited by either the depth resolution (in RBS), or possible errors introduced by the surface roughness of the processed polyimide samples which measured to be 300 A (in RT). Therefore, the measured diffusion coefficients appeared to

vary from technique to technique. Furthermore, metal clusters could be formed at the interface. They can affect the diffusion, but they are difficult to detect by techniques such as RBS and RT.

Optical second harmonic generation (SHG) with its high surface sensitivity allows a mechanistic study of metal cluster formation and diffusion into polymers by monitoring the signal in-situ and as a function of time.[10] It is known that SHG can be enhanced by metal clustering on surfaces and is sensitive to the size of metal grains at the surfaces. On the other hand, SHG will decrease if the metal clusters on the surface disappear into the polymer bulk by diffusion. Here we show how we can use SHG to study Cu cluster formation on polyimide, diffusion of Cu into polyimide, and formation of Cu/polyimide interfaces at different temperatures.[10] The samples were prepared by spin-coating polyimide material into a thin layer form (between 1 and 10 μm) on a glass plate. They were then annealed at 360 C in an inert gas to complete the imidization process. For the SHG measurement, a sample was mounted into an ultra-high vacuum (UHV) chamber with a base pressure of 1×10^{-9} torr. It was heated to 300- 360 C for several hours before copper was evaporated on the sample.

The SHG experiment was carried out by a commercial Q-switched and mode-locked YAG laser system (Quantronix 416) with output at 1.06 μm. The laser beam was slightly focussed onto the sample with a fluence less than 1mJ/cm. The incident angle was 75° from the metal side. The SH output in the reflection direction was detected by a photon counting detection system.

It is known that copper does not wet polyimide. Evaporation of Cu on polyimide would lead initially to Cu clusters. The same is true for Cu on glass. Because of surface local field enhancement, SHG from Cu clusters of few tens of nanometers in size can be two orders of magnitude stronger than that from a smooth Cu surface.[8,14] Figure 1 shows the SH signals from Cu on glass and polyimide during deposition as functions of effective thickness monitored by a quartz oscillator. Both data sets exhibit a maximum and then decay to approximately the same constant level towards large thickness. They can be understood as follows. Since Cu does not wet glass or polyimide in our case, the deposited metal atoms diffuse on the substrate, self-aggregate, and form clusters. When the clusters reach a size of a few tens of nanometers, they

strongly enhance SHG. With increasing metal deposition, the clusters gradually coalesce into a smooth continuous film; accordingly, SHG reduces to the level characteristic of a smooth metal surface.

We could deposit the same amount of Cu on polyimide at different temperatures and expect to find different Cu cluster distributions on the surface. This could be detected by SHG. For $T < T_g$ (T_g is about 320 C for our polyimide), we found that SHG from a sample with Cu deposited at a higher temperature was always stronger than that with Cu deposited at a lower temperature. The Cu deposition at the higher temperature must have created, on average, larger Cu clusters on polyimide due to the more rapid surface diffusion of Cu atoms and small clusters. At sufficiently high temperatures, Cu diffusion into polyimide became significant; larger Cu clusters would diffuse more slowly. This was confirmed by SHG measurements. In the experiment, the same amount of Cu (approximately a monolayer) was first deposited on two polyimide samples at two different temperatures, 150 and 250 C respectively. The samples were then heated within 1 min. to 300 C during which the Cu clusters hardly changed in size as monitored by SHG. Afterwards, the decay of SHG in time from the two samples kept at 300 C was observed as a consequence of diffusion of Cu clusters into the polyimide bulk, as shown in Fig. 2. The decay of SHG from the sample with Cu deposited at the higher temperature is indeed slower, indicating that larger Cu clusters diffuse more slowly into polyimide. By fitting the data in Fig. 2 with the solution of a one-dimensional diffusion theory, the diffusion constants for the cases can be derived.

Above T_g, the diffusion of Cu clusters into polyimide increased rapidly as seen from the increased decay rate of SHG from the sample. Obviously, polyimide is more permeable in the rubbery state. An example is presented in Fig. 3 where the diffusion constants of Cu clusters formed by evaporating 20 Å of Cu on polyimide at 300 C were deduced from SHG measurements from the sample at various temperatures above T_g. In the range between T_g(~320 C) and 460 C, they can be well described by the Arrhenius relation $D = D_0 \exp(-E_D/kT)$ with $D_0 = 5.1 \times 10^{-8}$ cm^2/s and $E_D = 1.2$ eV. Above T = 460 C, D increases much more rapidly. This coincides with

the incipient decomposition of polyimide, as evidenced by the change of color of polyimide from yellow to brown.

With the deposition of about a monolayer of Cu on polyimide at $T_g > T > T_{room}$, the formation of Cu clusters via surface diffusion on polyimide appeared to be near completion in a few minutes as monitored by SHG. This indicates that surface diffusion of Cu to form clusters must have dominated over Cu diffusion into the polyimide . When T was increased to approach T_g, the two processes became increasingly competitive. When T was above T_g, the maximum SHG generated was always very low, less than 20% of the maximum SHG generated at $T < T_g$, even after a massive amount of Cu was deposited. This indicates that diffusion of Cu into polyimide must have dominated over the cluster formation on the surface.

X-ray photoemission spectroscopic studies have suggested that Cu diffusion into polyimide can be blocked by a thin Ti buffer layer on polyimide.[15] This can be observed in situ by SHG. Figure 4 shows SHG versus time from two samples at 400 C: one with Cu deposited on a polyimide covered by 10 A of Ti and the other by 20 A of Ti. With the data of Fig. 2 as references, the effect of Ti is obvious. Clearly, one or two monolayers of Ti on polyimide are sufficient to effectively block Cu diffusion into polyimide. The result comes from the fact that Ti interacts strongly with both polyimide and Cu. With Ti completely covering polyimide, Cu atoms deposited on the surface are tightly bound to Ti and are no longer capable of diffusing. We have also observed from our SHG measurements that a layer of Cu clusters implanted into polyimide via diffusion from the surface has a similar blocking effect.

We now discuss how SHG can be used to probe alignment of liquid crystal (LC) monolayers on polymer surfaces,[16] which induces the bulk alignment. Surface-induced bulk alignment is a problem of great importance in the LC field. It is a process commonly adopted in the construction of almost all LC devices. Yet the physical mechanism responsible for the effect is not fully understood. For homogeneous alignment, mechanical rubbing of polymer-coated surfaces is often used. There are two possible mechanisms for the surface-induced bulk alignment. One similar to molecular epitaxy is based on short-range surface-molecule and then

molecule-molecule interactions to align the bulk.[17] The other assumes that mechanical rubbing creates grooves on the surface and the bulk alignment relies on minimization of long-range interaction (mainly elastic) between the surface and the bulk.[18] To see which mechanism dominates, we need to know how the first LC monolayer at the surface is aligned. The alignment is expected to be good if the molecular epitaxy mechanism is operative, but no so if the long-range mechanism is effective. Clearly such information can be obtained from SHG measurements on the LC monolayer at the surface.

The experimental arrangement is essentially the same as described earlier. We used four different input/output polarization combinations (p-in/p-out, p-in/s-out, s-in/p-out, and s-in/s-out) and measured the azimuthal dependence of SHG from reflection by rotating the sample about its surface normal. We first studies 8CB (octyl-cyanobiphenyl) monolayers on MAP (methylaminopropyltrimethoxy silane) - coated surfaces. With or without mechanical rubbing of the surfaces, the SHG signal is independent of the sample rotation, indicating that the monolayer orientation is azimuthally isotropic. The rubbed MAP-coated surface did yield homogeneous bulk alignment along the rubbing direction. The results therefore suggest that the alignment in this case must come from the above-mentioned long-range surface-bulk interaction.

The measurement on an 8CB monolayer adsorbed on polyimide-coated surface gave very different results. As shown in Fig.5, if the surface is unrubbed, the SHG signal is azimuthally isotropic, reflecting the azimuthal symmetry of the LC monolayer orientation. With rubbing, the data show a clear two-fold symmetry about the rubbing direction. From analysis of the data in Fig. 5, it is possible to deduce an approximate orientational distribution of the 8CB monolayer. First, from the theoretical fit of the data, the nonvanishing elements of the surface nonlinear susceptibility tensor $\chi^{(2)}$ for the 8CB monolayer can be deduced. These are $\chi^{(2)}_{zzz}$, $\chi^{(2)}_{xxx}$, $\chi^{(2)}_{zxx}$, $\chi^{(2)}_{zzx}$, $\chi^{(2)}_{zyy}$, and $\chi^{(2)}_{xyy}$ where x is along the rubbing direction, y in the surface plane, and z along the surface normal. Then, knowing how $\chi^{(2)}$ depends on the average molecular orientation in the monolayer, one can determine several weighted averages of the polar and azimuthal angles, θ and ϕ of the molecular orientation. By assuming a Gaussian distribution for the polar orientation,

$$P(\theta) \propto \exp[-(\theta - \langle\theta\rangle)^2/(\Delta\theta)^2]$$

and a serial distribution for the azimuthal distribution,

$$F(\phi) = [1 + a_1\cos\phi + a_2\cos 2\phi + a_3\cos 3\phi]/2$$

we can find $\langle\theta\rangle$, $\Delta\theta$, a_1, a_2 , and a_3. For the case of Fig. 5, we obtain $\langle\theta\rangle = 78^o$, $\Delta\theta = 10$, $a_1 = -0.13$, $a_2 = 0.69$, and $a_3 = -0.03$. The corresponding azimuthal distribution $F(\phi)$ is plotted in Fig. 6, which shows explicitly the rubbing-induced azimuthal anisotropy in the molecular orientational distribution. This anisotropy persists even when the monolayer is in contact with an isotropic bulk LC layer, although it is somewhat reduced, as depicted also in Fig. 6. Thus for the rubbed polyimide-coated surface, the surface-induced homogeneous bulk alignment must come mainly from the molecular epitaxy mechanism. As suggested by Patel and coworkers[17], rubbing aligns the polymer units at the surface of the polymer film. Interaction of the LC monolayer with the aligned polymer then leads to the anisotropic orientational distribution of the LC monolayer. Correlation between LC molecules finally produces the bulk alignment.

A few other polymers have been found to be effective for surface-induced bulk LC alignment.[16] SHG measurements have also confirmed the anisotropic distribution of LC monolayer alignment on such polymers when rubbed. These polymers all have the common property of being crystalline. Presumably, it is the crystalline property that allows the polymer surface to be stretched and aligned by rubbing.

Here we have considered only two examples of how one can use SHG to study relevant polymer interfacial problems. They are problems that cannot be studied by other means. One can certainly think of other interesting examples: for instance, the study of two-dimensional polymerization of a Langmuir monolayer,[19] and the study of surface memory effect imposed on polymers by an anisotropic medium.[20] Optical sum-frequency generation is expected to be even

more powerful as a surface analytical tool because it can provide spectroscopic information about polymer interfaces. This is, however, still an unexplored area. Applications of the technique to polymer interfaces will definitely open many exciting research opportunities.

This work was supported by the Director, Office of Energy Research, Office of Basic Energy Sciences, Materials Sciences Division of the U.S. Department of Energy under contract No. DE-AC03-76SF00098.

References

1. Y. R. Shen, *J. Vac. Sci. Technol.* B **3**, 1464 (1985); *Ann. Rev. Mater. Sci.* **16**, 69 (1986); *Nature* **337**, 519 (1989), and references therein.
2. More generelly, the surface and bulk of a medium have different structural symmetries and therefore the bulk contribution to a nonlinear optical process can be strongly suppressed by polarization descrimination.
3. N. Bloembergen and P. S. Pershan, *Phys. Rev.* **128**, 606 (1962).
4. F. Brown, R. E. Parks, and A. M. Sleeper, *Phys. Rev. Lett.* **14**, 1029 (1965); F. Brown and R. E. Parks, *Phys. Rev. Lett.* **16**, 507 (1966); N. Bloembergen, R. K. Chan, and C. H. Lee, *Phys. Rev. Lett.* **16**, 986 (1966); H. Sonnerberg and H. Heffner, *J. Opt. Soc. Am.* **58**, 209 (1968); G. V. Krivoshchekov and V. I. Stronganov, *Sov. Phys.-Solid State* **9**, 2856 (1968); *Sov. Phys.-Solid State* **11**, 89 (1969); N. Bloembergen, R. K. Chang, S. S. Jha, and C. H. Lee, *Phys. Rev.* **174**, 813 (1968); Erratum **178**, 1528 (1969).
5. N. Bloembergen and R. K. Chang, in *Physics of Quantum Electronics*, eds. P. L. Kelley, B. Lax, and P. E. Tannenwald (McGraw Hill, New York, 1966), p. 80; N. Bloembergen and Y. R. Shen, ditto, p. 119; J. Rudnick and E. A. Stern, *Phys. Rev.* B **4**, 4274 (1971).
6. F. Brown and M. Matsuoka, *Phys. Rev.* **185**, 985 (1969); J. M. Chen, J. R. Bower, C. S. Wang, and C. H. Lee, *Optics Comm.* **9**, 132 (1973); J. M. Chen, J. R. Bower, and C. S. Wang, *Jap. J. Appl. Phys. Supp.* **2**, 711 (1974).
7. M. Fleischmann, P. J. Hendra, and A. J. McQuillan, *Chem. Phys. Lett.* **26**, 163 (1974).
8. C. K. Chen, A. R. B. de Castro, and Y. R. Shen, *Phys. Rev. Lett.* **46**, 145 (1981).
9. C. K. Chen, T. F. Heinz, D. Ricard, and Y. R. Shen, *Phys. Rev. Lett.* **46**, 1010 (1981).
10. J. Y. Zhang, Y. R. Shen, D. S. Soane, and S. C. Freilich, *Appl. Phys. Lett.* **59**, 1305 (1991); J. Y. Zhang, Y. R. Shen, and D. S. Soane, *J. Appl. Phys.* **71**, 2655 (1992).
11. K. Shanker, J. R. MacDonald, *J. Vac. Sci. Technol.*, A **5**, 2894 (1987); J. H. Das and J. E. Morris, *Appl. Phys.* **66**, 5816 (1989).
12. R. M. Tromp, F. LeGeoues, and P. S. Ho, *J. Vac. Sci. Technol.* A **3**, 782 (1985).
13. F. Faupel, D. Gupta, B. D. Silverman, and P. S. Ho, *Appl. Phys. Lett.* **55**, 357 (1989).
14. A. Workaun, J. G. Bergman, J. P. Heritage, A. M. Glass, P. F. Liao, and D. H. Olson, *Phys. Rev.* B **24**, 849 (1981).
15. F. S. Ohuchi and S. C. Freilich, *J. Vac. Sci. Technol.* A **6**, 1004 (1988); P. O. Hahn, G. W. Rubloff, J. W. Bartha, F. LeGouse, R. Tromp, and P.S. Ho, *Mater. Res. Soc. Symp. Proc.* **40**, 251 (1985).
16. W. Chen, M. B. Feller, and Y. R. Shen, *Phys. Rev. Lett.* **63**, 2665 (1989); M. B. Feller, W. Chen, and Y. R. Shen, *Phys. Rev.* A **43**, 6778 (1991).
17. J. M. Geary, J. W. Goodby, A. R. Kmetz, and J. S. Patel, *J. Appl. Phys.* **62**, 4100 (1987).
18. D. W. Berreman, *Phys. Rev. Lett.* **28**, 1683 (1972); *Mol. Cryst. Liq. Cryst.* **23**, 215 (1973).
19. G. Berkovic, Th. Rasing, and Y. R. Shen, *J. Chem. Phys.* **85**, 7374 (1986).
20. Y. Ouchi, M. B. Feller, T. Moses, and Y. R. Shen, *Phys. Rev. Lett.* **68**, 3040 (1992).

Figure Captions

Fig. 1. SHG vs the effective thickness of Cu deposited on (a) polyimide and (b) silica glass at room temperature. (after Ref. 10.)

Fig. 2. SHG vs time from two Cu/polyimide sample at 300 °C with Cu deposited at sample temperature of (a) 250 and (b) 150 150 °C. Solid curves are theoretical fits from the solution of a one-dimensional diffusion equation using diffusion constants of (a) $D = 8 \times 10^{-19}$ cm^2/s and (b) $D = 2.5 \times 10^{-18}$ cm^2/s. (after Ref. 10.)

Fig. 3. Diffusion constant D vs inverse temperature 1/T for Cu cluster diffusion into polyimide. The solid line is a fit of the data between 320 °C (T_g) and 460 °C by the Arrhenius relation. (after Ref. 10.)

Fig. 4. SHG vs time from two Cu/Ti/polyimide samples at 400 °C with effective thickness of (a) 20 Å of Cu and 10 Å of Ti, and (b) 20 Å of Cu and 20 Å of Ti, and (c) 20 Å of Ti at 450 °C. (after Ref. 10.)

Fig. 5. Output second-harmonic field (arbitrary units) vs sample rotation Φ from 8CB monolayers on a polyimide-coaged substrate. Open squares are data from unrubbed substrates, filled circles are data from rubbed substrates, and solid lines are the theoretical fits. The input-output polarization combinations are (a) p-in/p-out; (b) s-in/p-out; (c) s-in/s-out. Inset: Coordinates (x,y,z) used in the analysis in relation to the fixed laboratory coordinates (X,Y,Z = z). The plane of incidence is $\hat{X}$-$\hat{Z}$. (after Ref. 16.)

Fig. 6. Amimuthal orientational distribution functions of an 8CB monolayer on a rubbed polyimide-coated substrate (solid line), and an 8CB interfacial layer between a rubbed polyimide-coated surface and an 8CB bulk (dashed line).

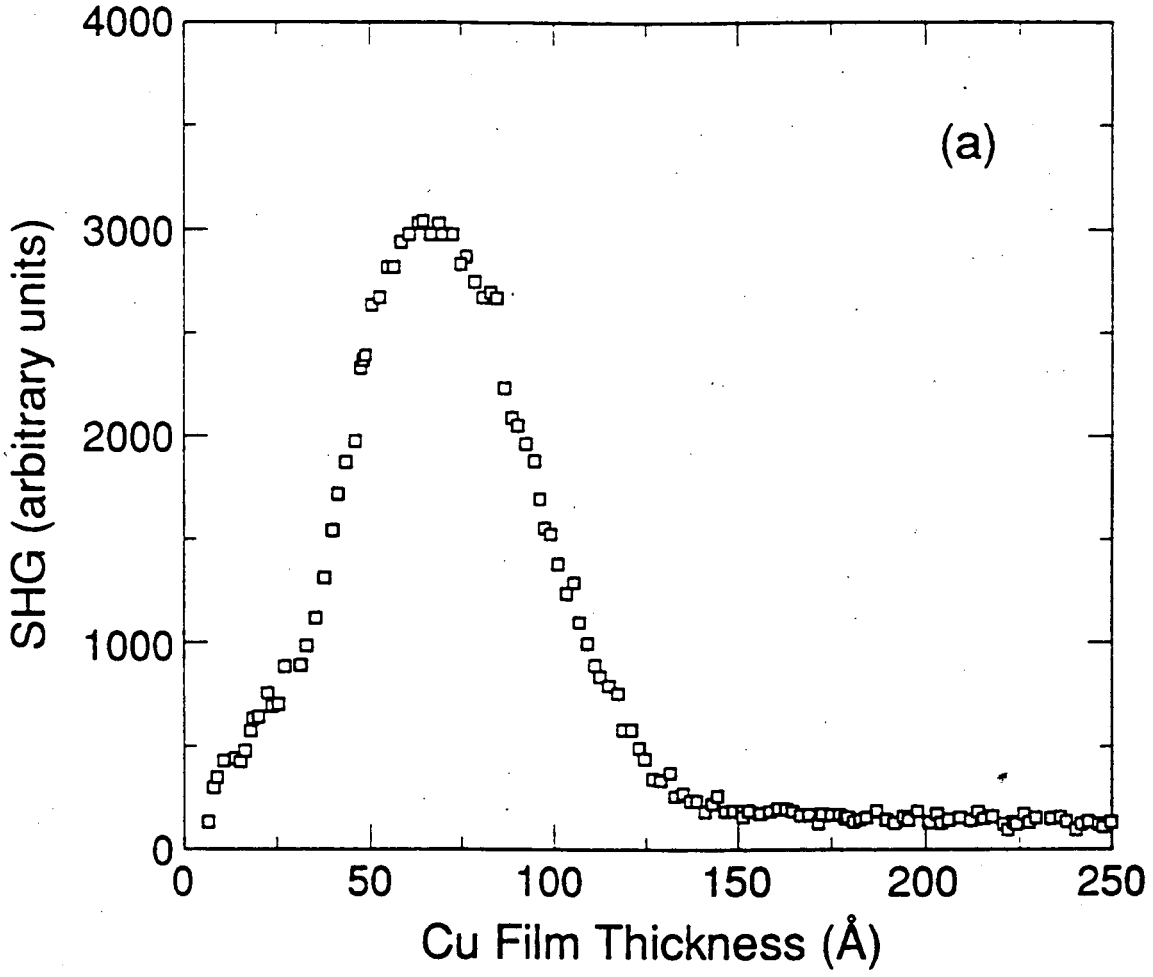

Y. R. Shen
Nonlinear Optical Studies of Polymer Interfaces
Fig. 1(a)

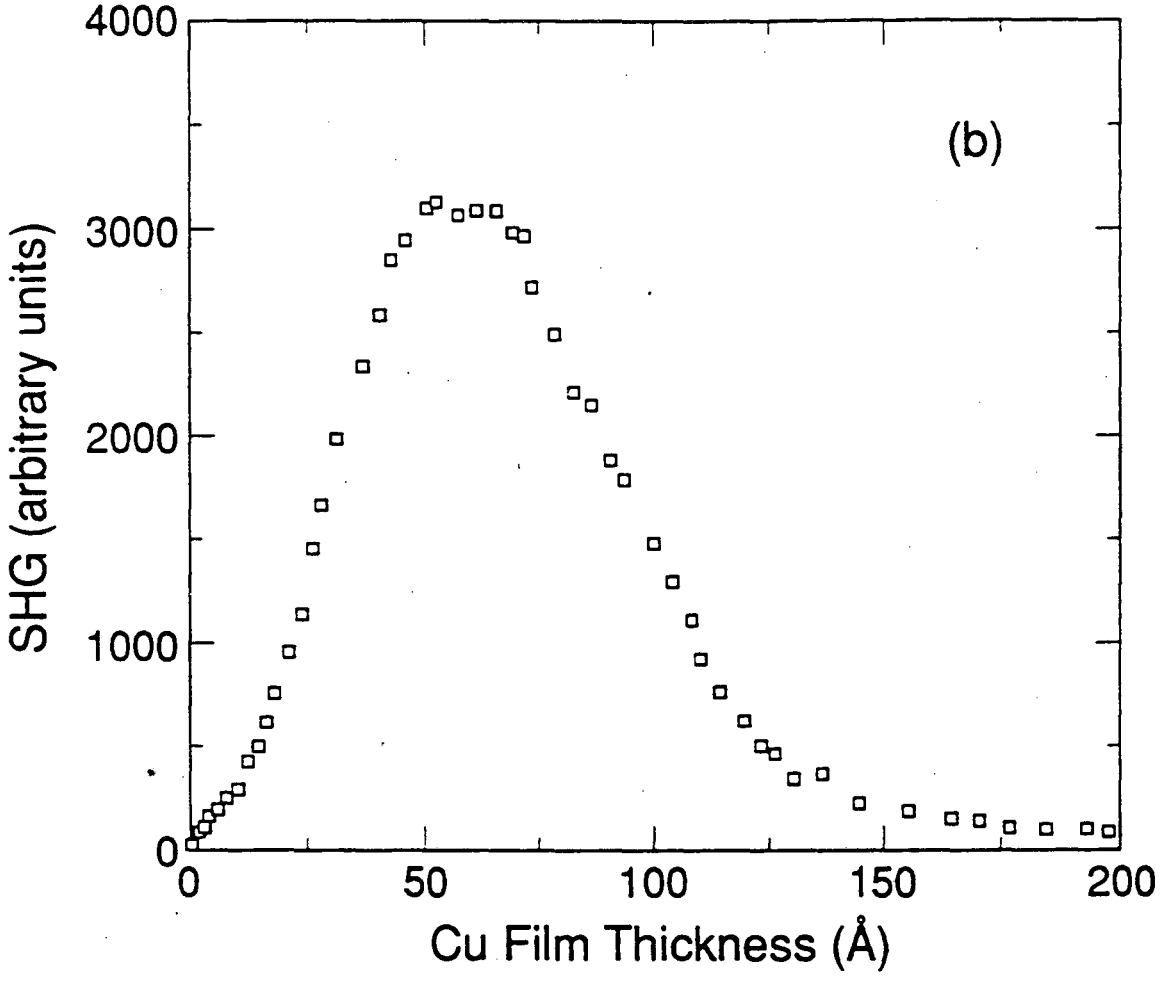

Y. R. Shen
Nonlinear Optical Studies of Polymer Interfaces
Fig. 1(b)

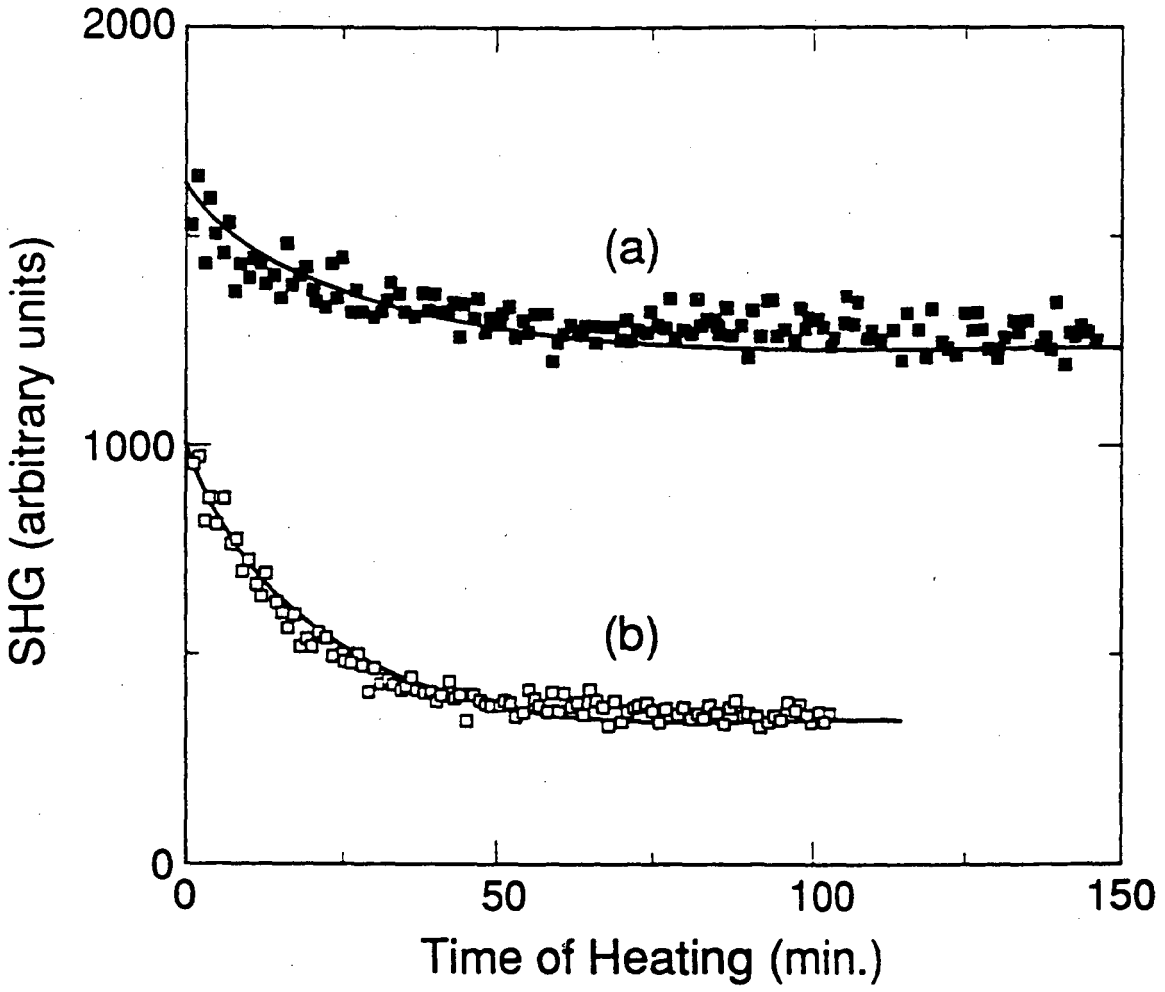

Y. R. Shen
Nonlinear Optical Studies of Polymer Interfaces
Fig. 2

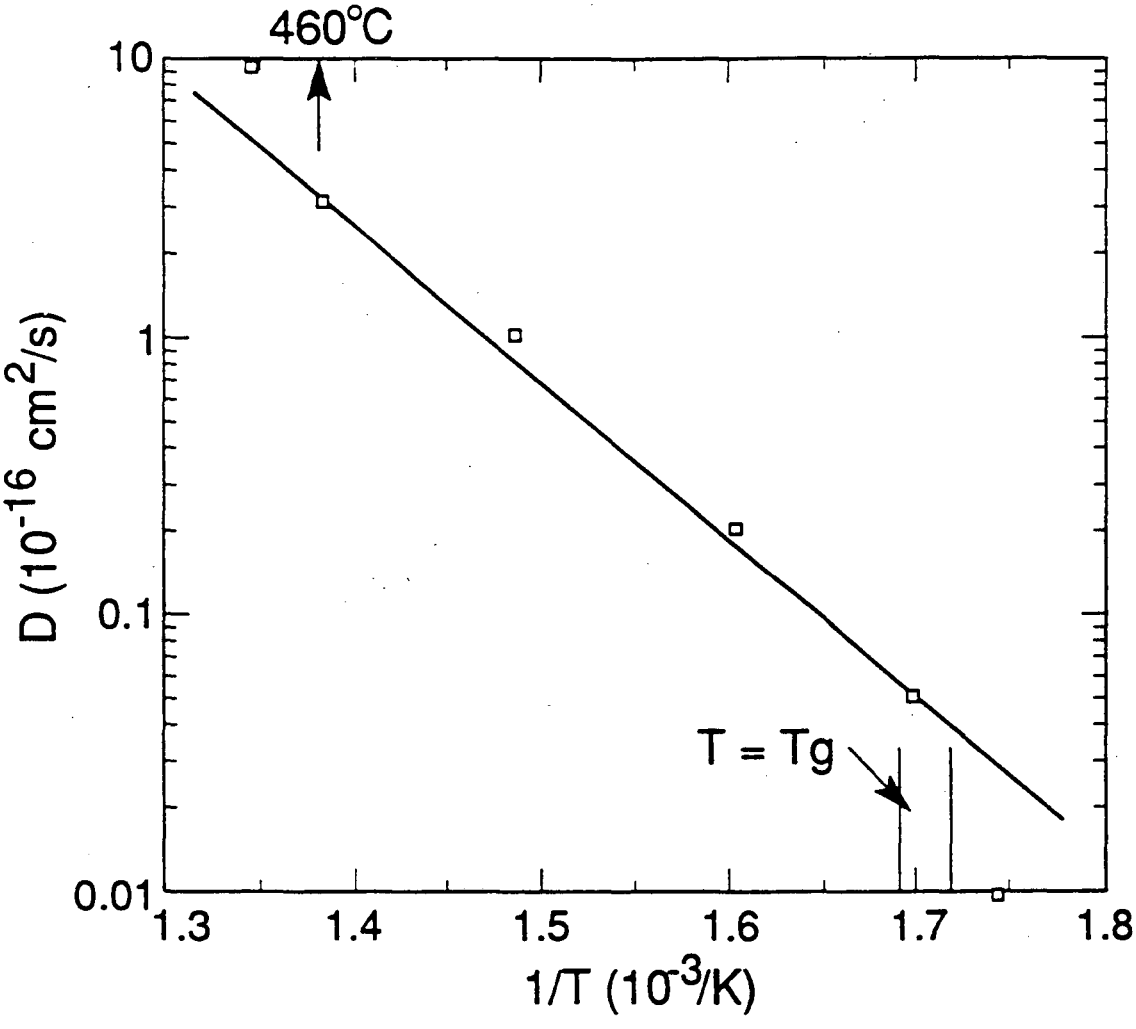

Y. R. Shen
Nonlinear Optical Studies of Polymer Interfaces
Fig. 3

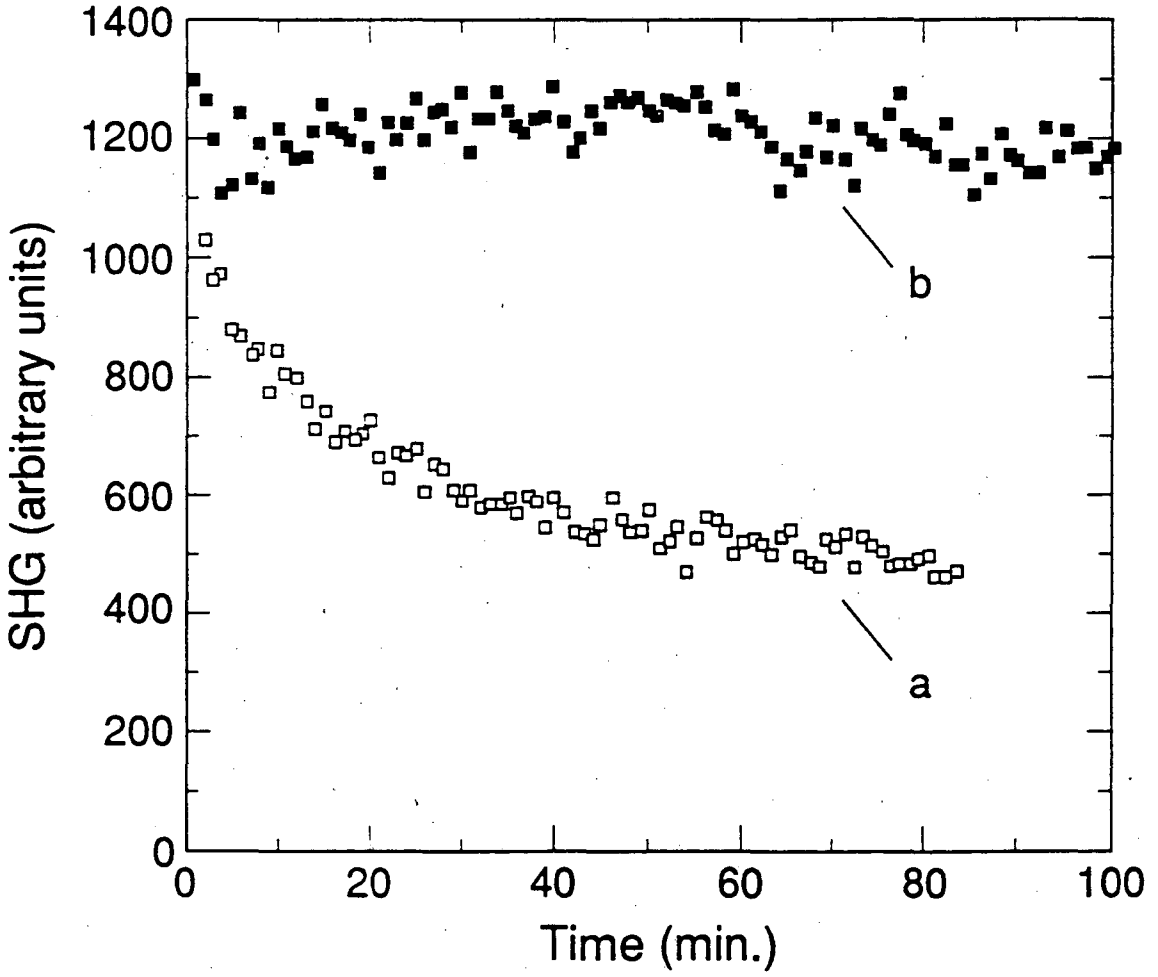

Y. R. Shen
Nonlinear Optical Studies of Polymer Interfaces
Fig. 4

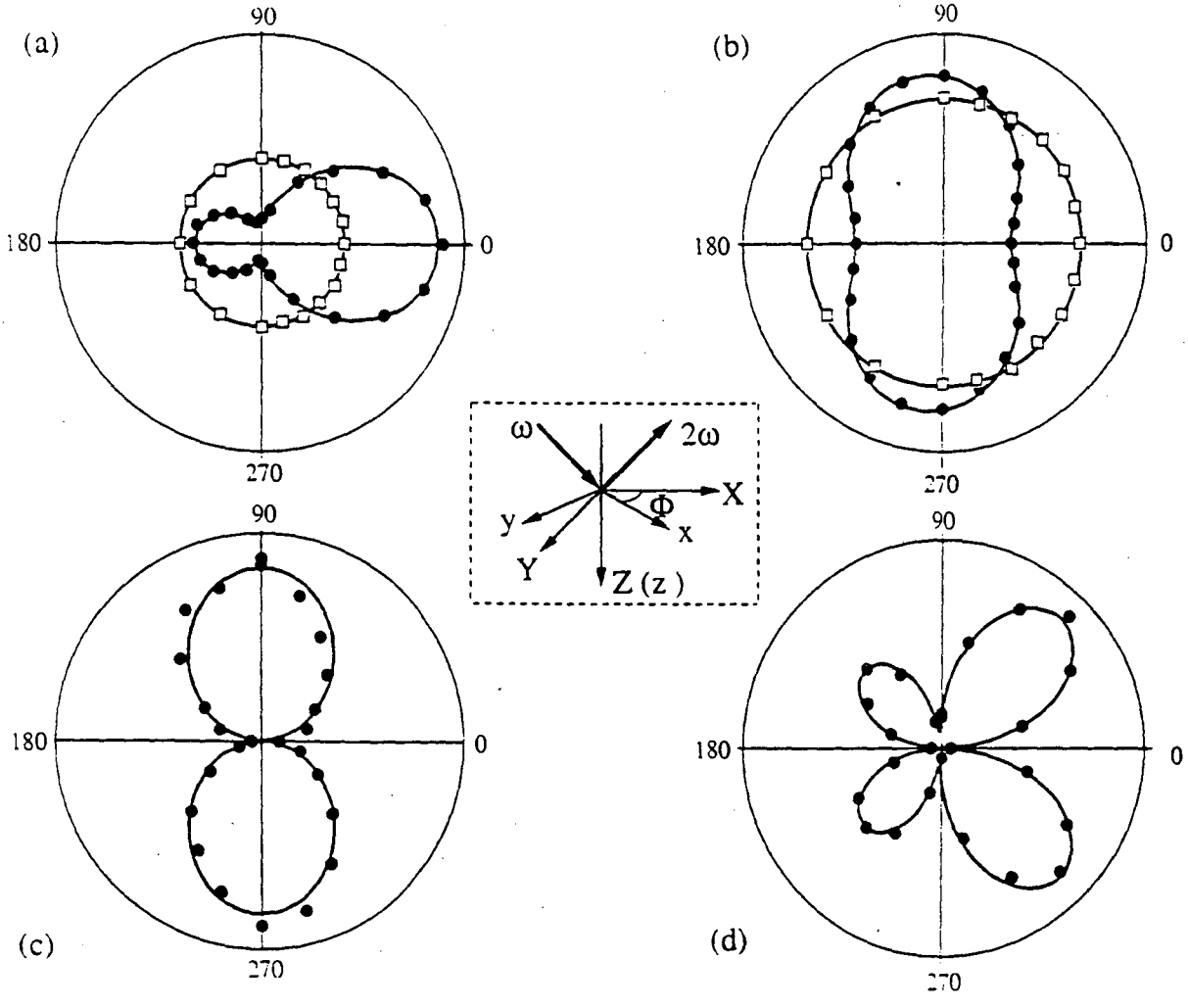

Y. R. Shen
Nonlinear Optical Studies of Polymer Interfaces
Fig. 5

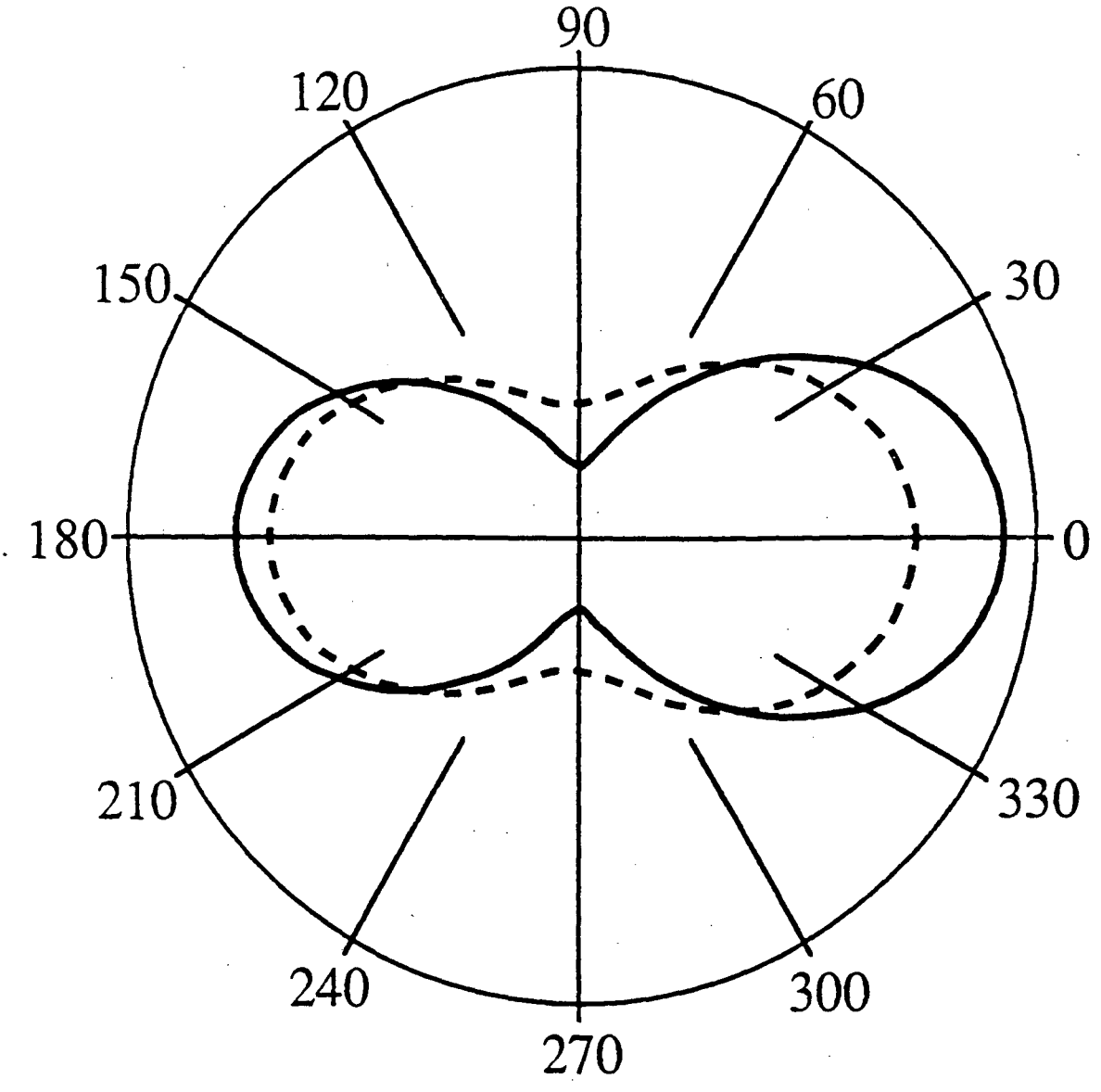

Y. R. Shen
Nonlinear Optical Studies of Polymer Interfaces
Fig. 6

LAWRENCE BERKELEY LABORATORY
UNIVERSITY OF CALIFORNIA
TECHNICAL INFORMATION DEPARTMENT
BERKELEY, CALIFORNIA 94720